ELSEVIER

Polymer 41 (2000) 675–683

polymer

Effect of repeat unit flexibility on dendrimer conformation as studied by atomistic molecular dynamics simulations

C.B. Gorman*, J.C. Smith

Department of Chemistry, North Carolina State University, Box 8204, Raleigh, NC 27695, USA

Received 20 November 1998; received in revised form 18 February 1999; accepted 24 February 1999

Abstract

The effect of repeat unit structure on the shape and internal organization of various dendrimers was probed using atomistic molecular dynamics simulations. In this technique, care was taken to ensure complete structural equilibration by implementing a high temperature dynamics/simulated annealing protocol prior to evaluation of the molecular structure and dynamics. Both flexible and stiff repeat units that have been employed previously in the synthesis of dendrimers were considered. Flexible-unit dendrimers were found to be globular but not completely spherical. In contrast, stiff-unit dendrimers had a more eccentric, disk-like shape. For all dendrimers, the different generations within each molecule were found to be radially distributed throughout its interior. This appearance could be attributed to back-folding of some of the repeat units in the flexible case and to a branching angle effect in the stiff case. This distribution, however, did not preclude a molecular surface composed of a substantial portion of the topologically terminal groups.

Keywords: Dendrimer conformation; Atomistic molecular dynamics simulations; High temperature dynamics

1. Introduction

The hyperbranched structure of dendrimers is now an increasingly precedented motif employed by researchers utilizing this architecture in applications such as molecular recognition [1–9], surface modification [10–20], asymmetric synthesis [21–27] and small molecule encapsulation [28–31]. It is of great interest to elucidate the geometric features of dendrimers such as their shape, size, and internal organization. To this end, a number of experimental and computational approaches have been devised to provide a physical picture of dendrimers including their overall shape and their internal structure. However, to date, this picture of dendrimer conformation is far from complete. Most notably, the effect of the primary structure of the dendrimer on its overall three dimensional structure has not been elucidated. Thus, little information is available for the development of rational design strategies and establishment of molecular structure–property relationships. Such information will be essential to the successful rational implementation of dendrimers in applications mentioned above.

A number of computations have been devised to elucidate dendrimer conformation. Initially, Lescanec and Muthukumar [32] reported kinetic-growth simulations predicting a density maximum at the topological center of dendrimer models with radially scattered branch ends at advanced stages of dendrimer growth (e.g. high generations). More recently, this general picture has been supported using coarse-grain molecular dynamics simulations (MDS) [33], coarse-grain Monte Carlo simulations [34–38] and coarse-grain self-consistent field calculations [39]. Likewise in these cases, repeat units closer to the topological periphery of the models were dispersed throughout the geometric interior of the model. These predictions have been confirmed in flexible molecules using REDOR NMR experiments on appropriately functionalized dendrons [40] and, more recently, by NMR relaxation studies on paramagnetic core dendrimers [41]. Coarse-grain models, however, treat molecules as a set of identical points interacting according to simple bonding and self-exclusion forces. Algorithms for evaluating their conformational manifold consider only basic enthalpic contributions arising from these generic bonding and self-exclusion energy terms. Atomistic MDS based on chemically specific potential energy terms would complement simplified models of the type cited above. To date, although the effect of the number of hyperbranches on molecular shape has been illustrated in one system using short, atomistic MDS [42] little additional structural information is available. The results mentioned above have been generated exclusively for dendrimers

* Corresponding author. Tel.: +1-919-515-4252; fax: +1-919-515-8920.

0032-3861/00/$ - see front matter
PII: S0032-3861(99)00167-6

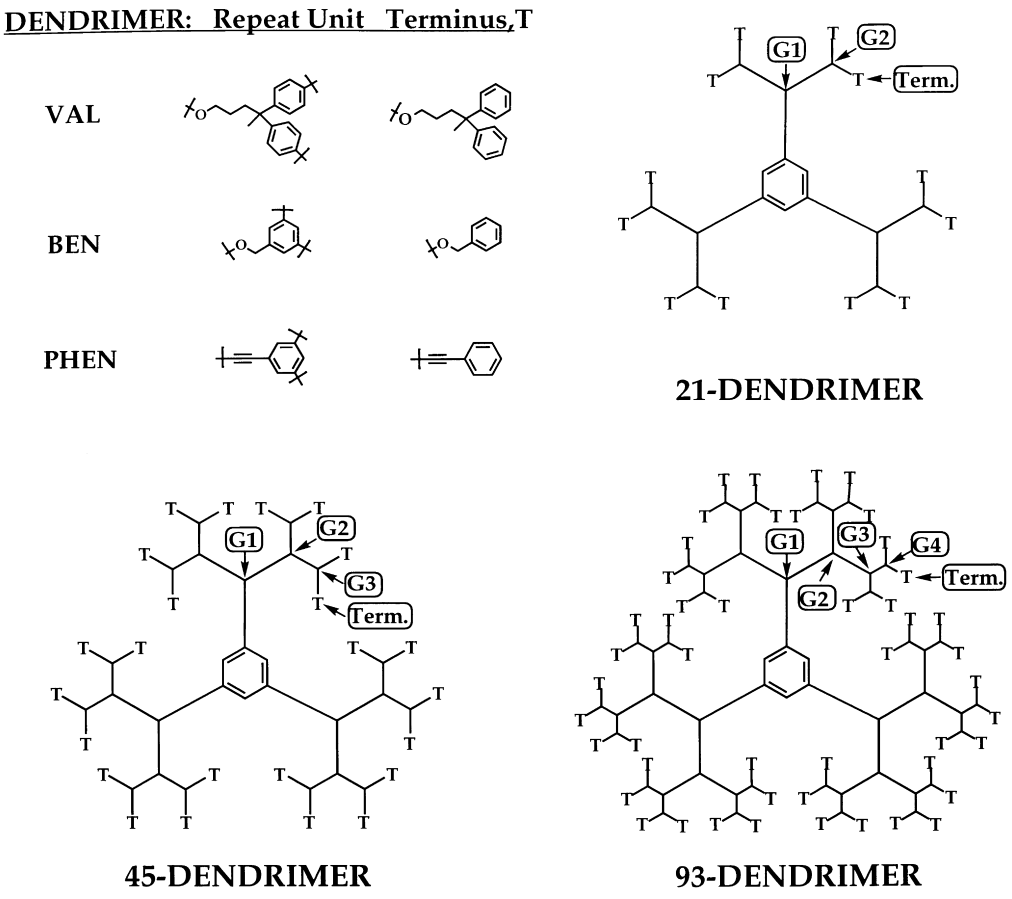

Fig. 1. Structures employed in this study. The numbers 21-, 45-, and 93- preceding the dendrimer label denote the number of repeat units in the structure. G1, G2, G*n* refer to the group of repeat units at the *n*-th hyperbranch point in the molecule. Term denotes the group of repeat units located at the topological periphery in each of the models.

composed of flexible units (i.e. those containing mostly low energy torsional barriers). High interior density due to molecular folding may or may not persist as the flexibility of the repeat unit is varied.

In this paper, the effect of conformational flexibility of a dendrimer repeat unit and generation (e.g. the number of hyperbranches within the molecule) on the overall geometry and organization of a dendrimer is studied using atomistic MDS. This relationship is explored over a size range of dendrimer models that are computationally feasible to equilibrate and constitute reasonable synthetic targets. Repeat units that are alternatively "flexible" and "stiff" are compared. These simulations were performed to augment the information obtained by the coarse-grain methods discussed above by providing a detailed atomistic picture of dendrimer conformation. A specific physical picture of shape and organization in the corresponding dendrimers is drawn.

2. Atomistic model and simulation method

All dendrimer models were built from monomers using the Builder module in the Biosym/MSI software and displayed using the INSIGHTII molecular visualization program. In order to simulate models in atomistic detail, interactions were defined according to the DISCOVER PCFF (version 3.0) all-atom forcefield. This forcefield incorporates the following potential terms:

$$\boldsymbol{E}_{\mathrm{Pot}} = \sum_{b}[K_2(b-b_0)^2] + \sum_{\theta}K_\theta(\theta-\theta_0)^2] + \sum_{\phi}K_\phi[1 + \cos(n*\phi-\phi_0)] + \sum_{\chi}K_\chi(\chi-\chi_0)^2 + \sum_{i>j}\frac{q_iq_j}{r_{ij}} + \sum_{i>j}\varepsilon_{ij}\left[2\left(\frac{r_{ij*}}{r_{ij}}\right)^9 - 3\left(\frac{r_{ij*}}{r_{ij}}\right)^6\right]. \quad (1)$$

The terms above are, respectively, the bond stretch term (b), the valence angle term (θ), the torsional potential (ϕ), the Wilson-out-of-plane potential (χ), a Coulomb term, and a Lennard-Jones 9-6 potential describing the van der Waals interactions where

$$r_{ij} = \left[\frac{r_i^6 + r_j^6}{2}\right]^{1/6} \quad (2)$$

and

$$\varepsilon_{ij} = 2\sqrt{\left(\varepsilon_i \varepsilon_j\right)} r_i^3 \frac{r_j^3}{\left[r_i^6 + r_j^6\right]}. \quad (3)$$

Forcefield parameters were taken from the PCFF version 3.0.0 forcefield. This forcefield is an extension of the consistent force field, CFF91 [43,44] and is designed explicitly for polymer and organic materials applications [45–47]. This forcefield is parameterized for polymer simulations and has comparably soft attractive interatomic van der Waals potential terms. This results in a better consistency with solution-state properties and is more representative, in principle, of Θ-solvent conditions than simulations performed using the CVFF forcefield which give more compacted, congested structures when used in the same protocol. Electrostatic interactions were calculated with a non-distance dependent dielectric constant of one. Functional groups that have been parameterized explicitly from quantum mechanics calculations and simulations include acetals, alcohols, alkenes, amines, carbonates, ethers, siloxanes, ureas, acids, alkanes, amides, aromatic groups, carbamates, urethanes, esters, silanes, and zeolites. No cross terms were taken into account.

As no X-ray or other structural data is available for dendrimers, the Insight II Builder module was used to construct the dendrimer models shown in Fig. 1. Each of these dendrimer models were constructed in a completely extended conformation (e.g. dihedral angles set to 180°). After construction of a model, the structure was minimized to RMS < 0.01 kcal mol^{-1} Å^{-1}. In so doing, bonds were relaxed to their respective equilibrium bond distances. Next, the BEN- and VAL-derived structures were subjected to 100 ps of 600 K constant temperature dynamics to search for and obtain a low energy, equilibrium conformation for each structure [48,49]. The PHEN-derived structures were subjected to a preheating schedule before this procedure to avoid shocking. Subsequently, the temperature was stepped down in 50 K increments to 50 K. At each temperature step, atom velocities were readjusted and 5 ps of constant temperature molecular dynamics was performed. At 50 K, each structure was then minimized using steepest descents/conjugate gradients to RMS < 0.001 and equilibrated for 45 ps at 273 K. A 500 ps production trajectory at 273 K was then obtained. Computations were also performed using the CVFF forcefield. However, the use of the CVFF forcefield gave unrealistically compact dendrimer structures and occasionally failed to reach an equilibrium structure in the simulated annealing procedures described below. These behaviors were traced to the large attractive interatomic van der Waals forces inherent in this forcefield parameterization.

In all cases, constant temperature was achieved by direct velocity scaling as described below. During production dynamics, every structure had a constant average potential energy history consistent with an equilibrium structure. Similar results were obtained when other, arbitrary starting conformations were employed in the equilibration procedure and when the structures were subjected to multiple annealing cycles, suggesting that rigorous equilibration had been achieved.

During the annealing schedule, bonds were constrained to their equilibrium bond lengths using the RATTLE algorithm [50]. By applying constraints to bonds, the assumption that atom velocities and accelerations are constant becomes valid for large integration timesteps. In this way, a relatively long integration timestep of 2 fs was used without introducing instability or inaccuracy in the integration process. In addition, long range van der Waals interactions were neglected beyond a certain point, specified by the "cutoff distance". Inaccuracy and instability may be introduced in this way as well due to discontinuities in energy derivatives. The DISCOVER 3.0.0 program incorporates a switching function to remedy the abrupt cutting off of non-bonded interactions. The switching function is mathematically incorporated into the forcefield and effectively smoothes the van der Waals potential from its natural potential energy to zero over a specified interval. This interval is specified by a parameter in the simulation, swtdis. In addition, since atoms are continually changing their relative positions throughout the simulation, a protocol for updating atom neighbor lists is incorporated. This protocol involves the definition of a distance range outside the cutoff distance, called the buffer width, within which atom lists are updated before every integration step. The buffer width is explicitly specified in DISCOVER 3.0.0. In all calculations, non-bonded interactions were cut off at 9.5 Å (cutoff = 9.5 Å), the switching function was applied over the last 1.0 Å (swtdis = 1.0 Å), and the buffer width was 0.5 Å outside of the cut off distance.

In all simulations, initial velocities were generated so as to maintain a Maxwell–Boltzmann distribution at a specified "temperature". During dynamics kinetic energy is constantly changing to potential energy and vice versa. To maintain the correct temperature, atom velocities must be scaled periodically. In all simulations, "direct velocity scaling" was employed for this purpose. In contrast to other methods that, for example, adjust single atom velocities according to a Boltzmann distribution at every integration step, direct velocity scaling uniformly scales all atom velocities at one time according to the equation:

$$\left(\frac{v_{\text{new}}}{v_{\text{old}}}\right)^2 = \frac{T_{\text{target}}}{T_{\text{system}}}. \quad (4)$$

This scaling occurs only if the temperature of the system changes more than 10 K between two integration steps and is explicitly specified within the DISCOVER 3.0.0 program as the parameter, "temperature window".

Radial density distribution functions ($g(r)$) and mean square displacement correlation functions (MSD⟨Å^2⟩) were averaged over the 500 ps production trajectory. Radial

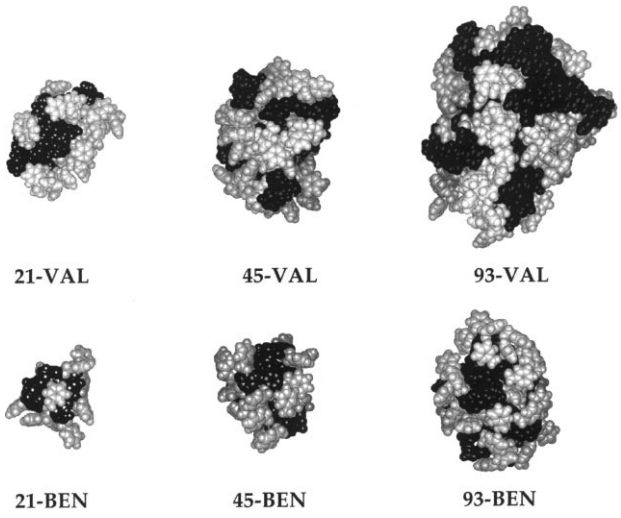

Fig. 2. CPK models of VAL- and BEN-derived dendrimers obtained at the midpoint of the 500 ps production dynamics run. Repeat units at the terminus (Term) are colored light gray. All others are colored black.

density distribution functions denote the density of atom centers in a 0.01 Å thick radial shell centered at a radial distance, r, from the dendrimer core. Number density distribution functions ($\langle N(r)\rangle$) were generated by multiplying $g(r)$*shell volume, and denote the number of atom centers at radial distance, r, from the dendrimer core. Aspect ratios are ratios of the principal moments of inertia, (Iz/Ix) where $Ix < Iz$. Surface accessible repeat units were analyzed by soaking (no equilibration) the models in a set of chloroform solvent molecules, and listing repeat units within 4.5 Å from any solvent molecule.

3. Results and discussion

3.1. Structures under consideration

A series of MDS was performed to compare and contrast the shape and internal organization of different dendrimers with repeat units that were alternatively flexible and stiff. To maximize the practical utility of these computations, repeat units commonly reported in the literature were chosen. This approach does not merely indicate the effect of repeat unit stiffness on overall structure as these molecules have other differences. Variation of repeat unit flexibility by, for example, artificially changing a torsion barrier in the forcefield employed would permit a continuous mapping of this parameter on overall dendrimer structure. However, such results cannot be correlated in a straightforward fashion with real chemical systems. Thus, the former method has been employed here.

The structures of the dendrimers under study are depicted in Fig. 1. The designation “generation” is used here to refer to a topological group of repeat units within a given dendrimer. Thus, generation 1 (G1) refers to the three repeat units covalently bonded to the benzene core of the molecule. In a similar fashion, generation n (Gn) refers to daughters covalently bonded to G$n-1$. Molecules are referred to by the number of repeat units in the structure (e.g. 21DENDRIMER, 45DENDRIMER, and 93DENDRIMER). Dendrimers based upon the units termed BEN (for a 3,5-dibenzyloxy repeat unit) [51,52] and VAL (for a 4,4′-diphenyl-isovaleroxy repeat unit) [53] have been reported previously by Fréchet’s group. These two units were chosen to represent flexible repeat unit dendrimers. The VAL unit is more flexible than the BEN unit because of the greater number of low energy torsions in its methylene chain. It is

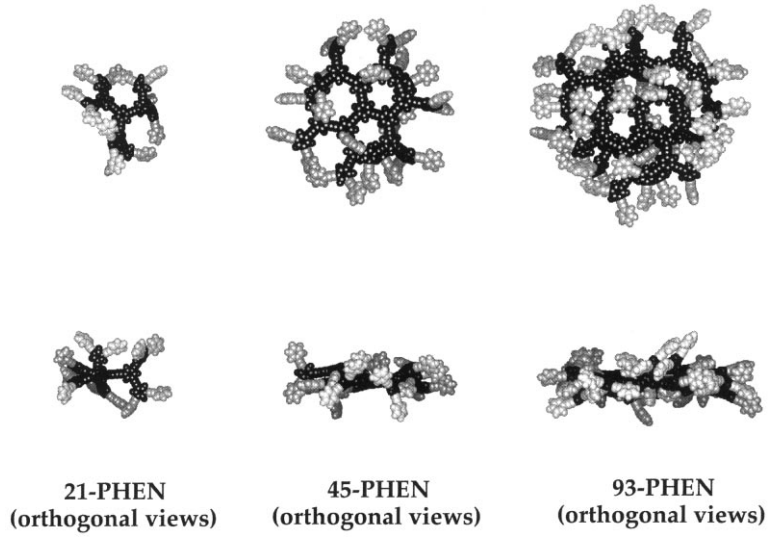

Fig. 3. CPK models of PHEN-derived dendrimers obtained at the midpoint of the 500 ps production dynamics run. Repeat units at the terminus (Term) are colored light gray. All others are colored black. Orthogonal views of each model are presented.

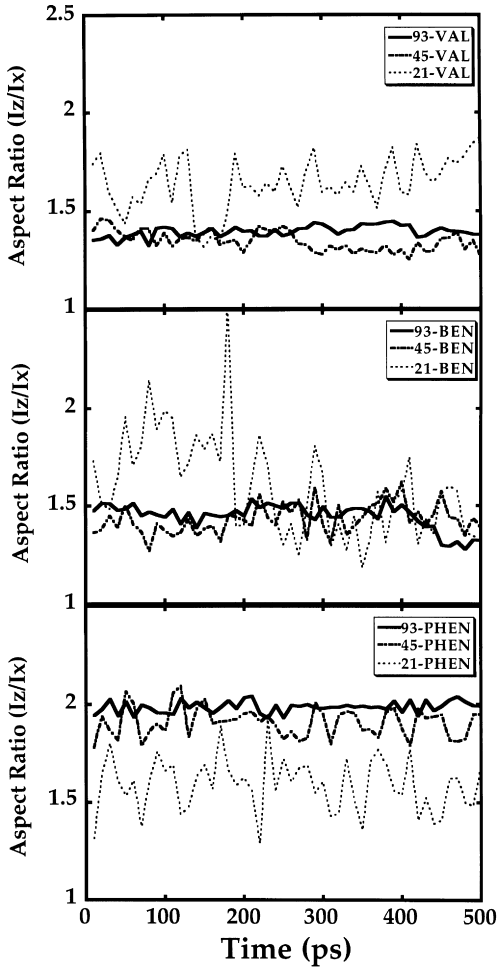

Fig. 4. Aspect ratios (*Iz*/*Ix*) of the models tabulated during the course of production dynamics.

also larger than the BEN unit and thus gives an indication of how molecular weight influences dendrimer structure for molecules with the same number of hyperbranches. Dendrimers based upon the PHEN unit have been reported previously by Moore's group [54–57] and were chosen to represent a rigid repeat unit dendrimer. All of these units have no specially designed features such as hydrogen-bonding or extreme steric bulk within the units. Such features may have notable effects on the overall shape and organization of the dendrimer. These effects are not treated here.

The core of the dendrimers studied here was chosen to be a 1,3,5-trisubstituted benzene moiety. Although not all of the dendrimer molecules reported in the literature had this core, it was used here so as not to bias the observed differences in the dendrimers studied by an additional variable. We hope to specifically illustrate the effect of the coordination number and symmetry of the dendrimer core on its overall shape and organization in future work.

3.2. Molecular shape

The rigidity of the repeat unit has been suggested to be a dominant factor in controlling dendrimer shape [56,58–62]. The results of the simulations reported here are also consistent with this hypothesis. These shapes are illustrated in a static sense using CPK models of these dendrimers in Figs. 2 and 3. These models are snapshots of the molecules at the midpoint of the production dynamics and were representative of the shapes of the molecules during the course of the simulations. In these depictions, the terminal groups of each dendrimer are shaded lighter than the other groups. The significance of these distributions will be discussed in Section 3.4.

The globular shapes found for the BEN and VAL dendrimers resulted from contraction of dendron arms around the topological core. This contraction was driven by interatomic van der Waals interactions as evidenced by a large change in the dispersive van der Waals energy component of the total energy expression during relaxation. Boris and Rubinstein have previously discussed the entropic favorability of this behavior [39]. The results presented here, however, are consistent with those generated using statistically rigorous coarse-grain models that consider entropy [33–39]. The dynamic shape of these dendrimers was illustrated by plotting their aspect ratio (e.g. calculated from principle moments of inertia, *Iz*/*Ix*, Fig. 4) as it evolved during the course of the production phase of the simulation. The smallest flexible dendrimers (21-BEN and 21-VAL) exhibited a large apparent change in shape during the course of the simulation. This change was due to substantial motion of the peripheral groups in these molecules. In these small molecule cases, the peripheral groups made up a substantial portion of the molecule and were not crowded. In addition, the average aspect ratio of 21-BEN and 21-VAL over the course of the simulation was large compared to the larger BEN- and VAL-derived flexible dendrimers. The molecules 45-BEN, 45-VAL, 93-BEN, and 93-VAL exhibited a more or less constant aspect ratio of approximately 1.4 which is consistent with an eccentric spheroid, globular shape. This change in aspect ratio with increasing generation is consistent with experimental predictions of a change from a more extended to a more globular shape at approximately this degree of hyperbranching [63–66]. For the larger molecules, these observations indicate that flexible repeat unit dendrimers exhibit a compact, space-filling structure in both a static and dynamic sense. We have illustrated this effect more specifically via MDS on BEN-derived dendrimers [67].

Unlike dendrimers derived from the flexible repeat units VAL and BEN, PHEN-derived dendrimers exhibited a very different shape. These dendrimers were much more disk-like as evidenced by the static CPK models in Fig. 3 and the aspect ratios in Fig. 4. The molecule 21-PHEN exhibited a larger change in shape over the course of the simulation, again due to substantial motion of the peripheral groups. However, 45-PHEN and 93-PHEN had a more or less constant aspect ratio of 1.8–1.9, consistent with the disk-like conformations shown in Fig. 3. Note that these

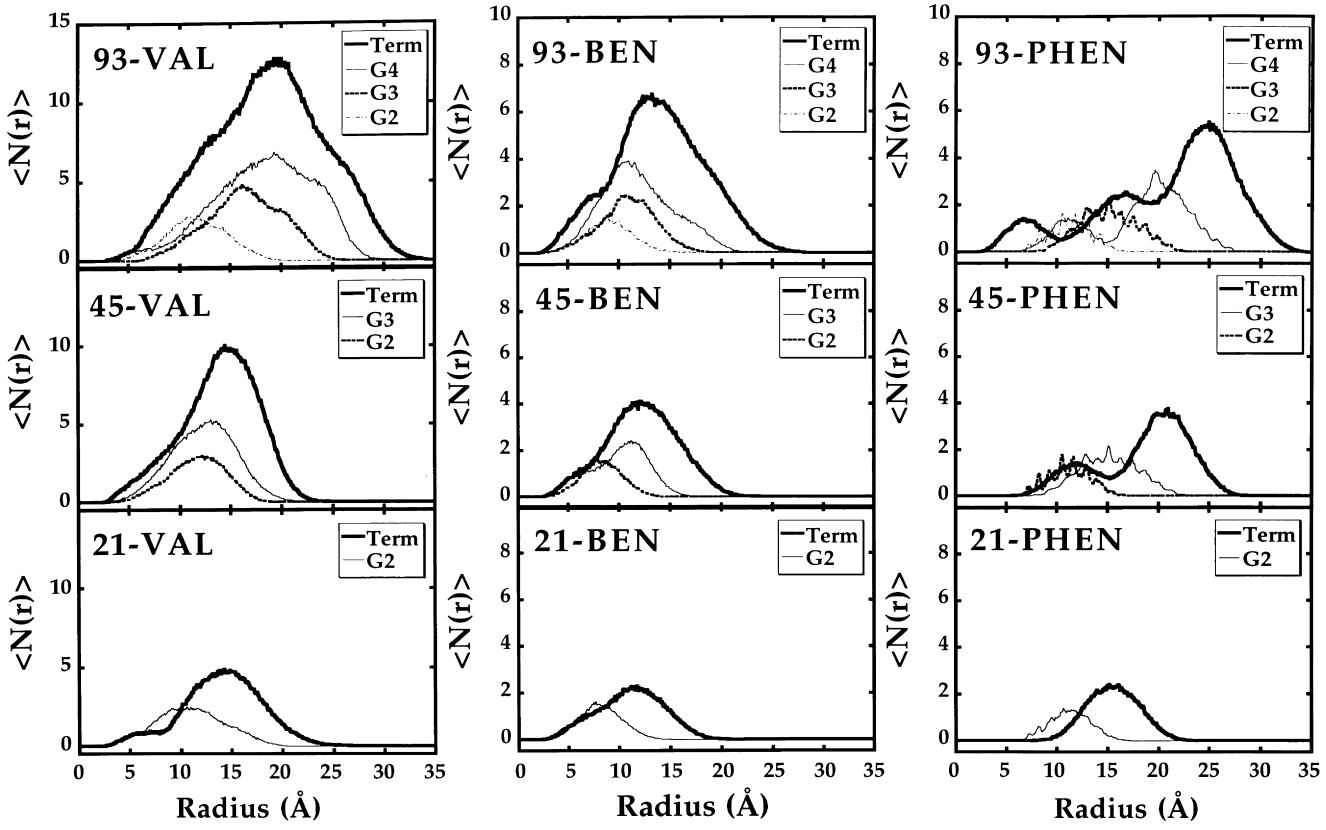

Fig. 5. Number density distribution functions ($\langle N(r)\rangle$) averaged over 500 ps of production dynamics for each dendrimer model.

conformations were obtained after high temperature annealing was performed on structures in which the dendrimers were initially placed into a *spherically symmetric* conformation around the central benzene core. The energetic driving force for assuming this shape is attractive interatomic van der Waals forces that are optimized by concentrating phenylacetylene repeat units in a single plane. Energetically favorable π-conjugation among phenyl rings is also afforded by a planar conformation and is incorporated in the parameterization of the forcefields employed. Electron microscopy and powder diffraction data on crystalline phenylacetylene macrocycles and small dendrimers support a planar orientation of these molecules in the condensed state [61]. In addition, Monte Carlo conformational searching on rigid polyphenylene dendrimers indicated planar, low energy conformations for these rigid molecules [62].

3.3. Internal organization

In addition to shape, the internal organization of the dendrimer units is important in developing molecular design rules. The spatial distribution of repeat units throughout each dendrimer was determined by computing number distribution functions (NDFs) for each of the molecules under study. These functions (Fig. 5) represent the number of atoms at a given radial distance from the molecular core and were calculated for atom centers in each set of topologically identical repeat units (labeled as indicated in Fig. 1). The values of these functions are those averaged over the course of the 500 ps production trajectory.

The NDFs for each of the three types of dendrimers illustrate that each topological generation was distributed throughout the geometric interior of each molecule. This trend was found for both the flexible and stiff dendrimers. In the case of flexible dendrimers, this distribution was attributed primarily to folding within the units of the molecule. This folding motif has been illustrated in most previously performed, coarse-grained computations of dendrimer conformation [33–36,38,39]. Dendron folding in the condensed and solution-state has been indicated experimentally. Solid-state REDOR NMR on flexible dendrons indicated close contact between the focal and peripheral groups within individual molecules [40]. Examination of longitudinal NMR relaxation times in paramagnetic core dendrimers also indicated close approach of all units within a dendrimer to the molecular core [41].

It was initially surprising to find NDFs for the stiff PHEN-derived dendrimers that were qualitatively so similar to those found in the flexible dendrimers. On first glance (Fig. 5) NDFs for 93-PHEN and 45-PHEN had some periodicity. This observation was easily rationalized by the geometrical constraints imposed by the stiff repeat units. It is also notable that topological generations within each molecule (excluding 21-PHEN in which they are more

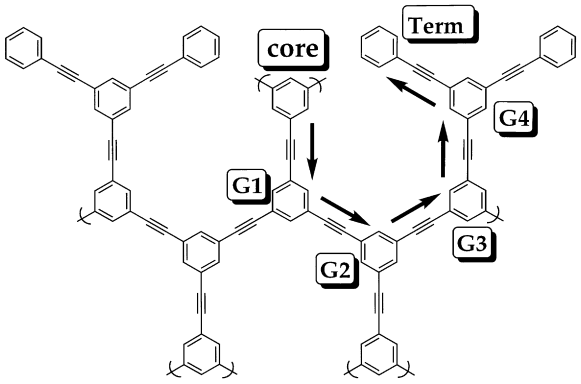

Fig. 6. Schematic depicting the "inward folding" of stiff-chain dendrons via a rigid branching angle that forces repeat units in toward the molecular core.

radially localized) were radially disposed throughout each molecule. This disposition could not be due to folding within these molecules as none of the linkages should permit this. Rather, it was attributed to the angle of hyperbranching in the molecules. At each hyperbranch after the first one, the angle of branching splays one half of the groups in towards the center of the molecule. This hyperbranching effect is illustrated schematically in Fig. 6. This schematic predicts a high density of terminal repeat units should be found near the molecular core after four hyperbranches (e.g. for 93-PHEN). Indeed this was observed. The radial density distribution functions ($g(r)$, Fig. 7) for the PHEN-derived dendrimers emphasizes this high local density in 93-PHEN compared to the smaller 45-PHEN and 21-PHEN. Simply, this molecule contains the requisite number of hyperbranches to bring the terminal groups around to the molecular core. Recently, a dramatic shift in fluorescence λ_{max} was observed in PHEN-derived dendrons with this number of hyperbranches when compared to smaller dendrons [68]. This topological explanation might rationalize these experimental data.

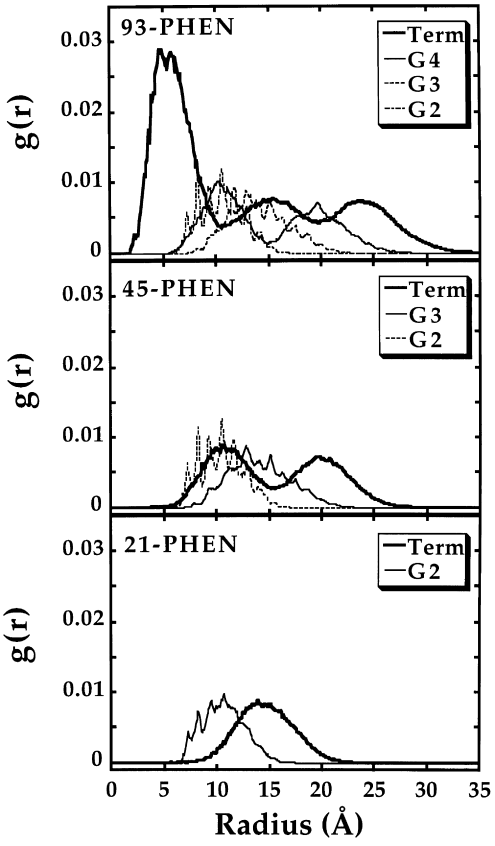

Fig. 7. Radial density distribution functions, $g(r)$, for PHEN-derived dendrimer models emphasize sudden density increase for 93-PHEN in the core region due to "inward folding."

3.4. Composition of the geometric periphery

Although all of the generations within each dendrimer are found to be radially distributed throughout the molecule, this conformation does not preclude finding a number of the topologically terminal groups at the geometric exterior of each molecule. The composition of the exterior surface of dendrimers is important for catalysis and molecular recognition applications. To indicate the composition of the exterior of the dendrimers, the CPK models in Figs. 2 and 3 were color-coded to discriminate terminal (light gray) from nonterminal (black) repeat units. In the case of PHEN-derived dendrimers, their disk-like shape placed the majority of the repeat units at the accessible surface of the molecule. Thus their molecular surface was not found to be dominated by any particular topological generation. In contrast, the surfaces of the VAL- and BEN-derived dendrimers were found to consist of a substantial number of terminal groups. The number of repeat units in each of the generations at the surface of each molecule was tabulated over the course of production dynamics (Fig. 8). This analysis revealed that ca. 40 of the 48 terminal repeat units were found at the periphery in both 93-VAL and 93-BEN. This observation does not preclude finding a number of interior groups (G2–G4) at the surface of these molecules. Fig. 8 illustrates that, indeed, a number of the interior groups were found at each molecular surface over the course of production dynamics. These observations indicate a structure in which most of the branch ends are concentrated at the surface of each dendrimer, yet a number are dispersed in the molecular interior.

This distribution of repeat units was also reflected by their relative mobility. This mobility is illustrated for 93-VAL 93-BEN, and 93-PHEN by computing the average atomic mean square displacement correlation functions of each generation within each molecule over the course of production dynamics (Fig. 9). The terminal groups in each molecule were, on average, substantially more mobile than the other generations on this time-scale. This behavior can be attributed to decreased steric congestion at the surface of 93-BEN and 93-VAL and to decreased steric congestion at the periphery of the disk in 93-PHEN. Conversely, the reduced average mobility of the other generations was

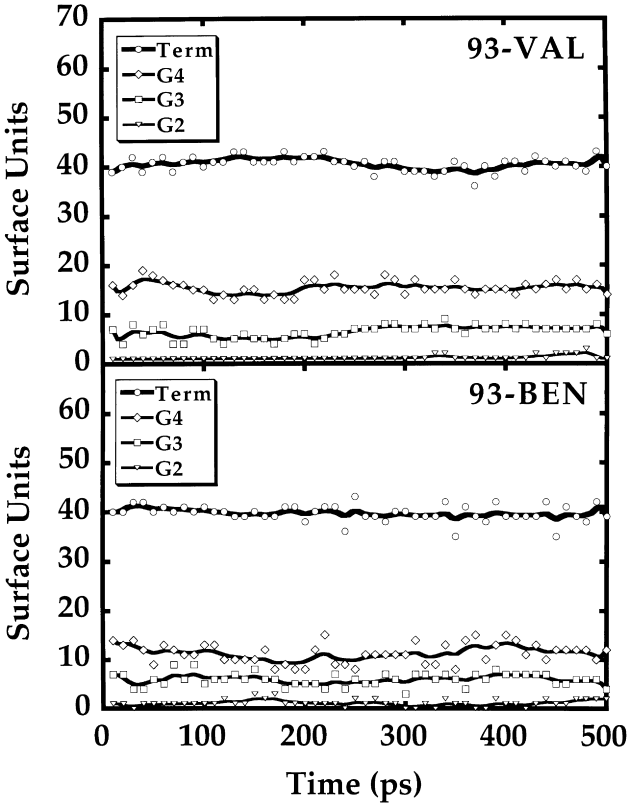

Fig. 8. Surface accessible repeat units for 93-DENDRIMERS categorized by generation.

attributed to their prevalence in the more densely packed interior.

4. Conclusions

Atomistic MDS on equilibrated dendrimer structures illustrated differences in shape and internal organization of dendrimers as the flexibility of the dendrimer repeat unit was varied. In general, flexible repeat unit dendrimers possessed a somewhat eccentric but globular shape. Stiff-chain (phenylacetylene) repeat unit dendrimers were, in contrast, more disk-like in shape. For all dendrimers, the different generations within each molecule were found to be radially distributed throughout its interior. This appearance could be attributed to back-folding of some of the repeat units in the flexible case and to a branching angle effect in the stiff case. This distribution, however, did not preclude a molecular surface composed of a substantial portion of the topologically terminal groups.

Acknowledgements

This research was supported by NC State startup funds, the Air Force Office of Scientific Research MURI program in Nanoscale Chemistry and by the National Science Foundation (CAREER Award, DMR-9600138).

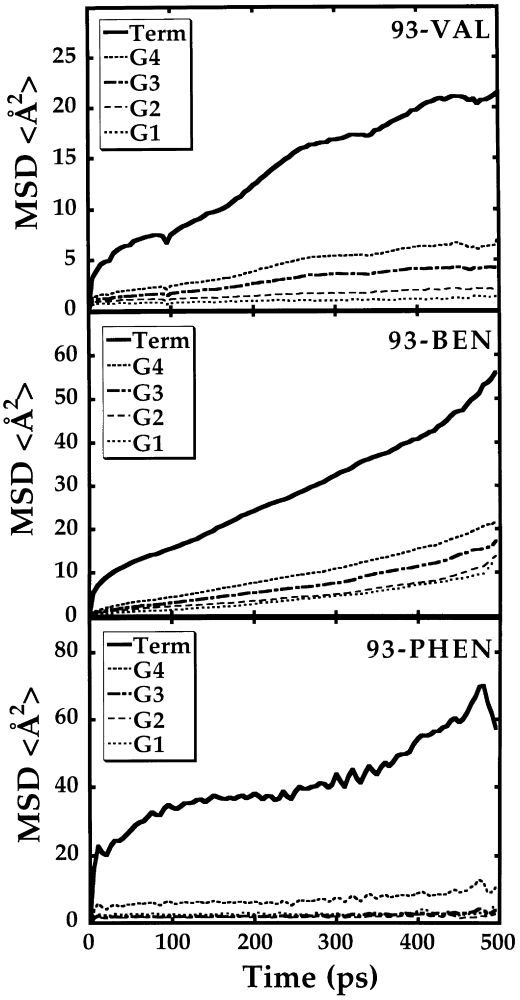

Fig. 9. Averaged atomic mean square displacement correlation functions (MSD⟨Å^2⟩) for repeat units in the 93-DENDRIMERS categorized by generation.

References

[1] Zeng F, Zimmerman SC. Chem Rev 1997;97:1681–1712.
[2] Zanini D, Roy R. J Am Chem Soc 1997;119:2088–95.
[3] Walliman P, Seiler P, Diederich F. Helvetica Chim Acta 1996;79:779–88.
[4] Valério C, Fillaut JL, Ruiz J, Guittard J, Blais JC, Astruc D. J Am Chem Soc 1997;119:2588–9.
[5] Turro NJ, Barton JK, Tomalia DA. Acc Chem Res 1991;24:332–340.
[6] Newkome GR, Woosley BD, He E, Moorefield CN, Güther R, Baker GR, Escamilla GH, Merrill J, Luftman H. Chem Commun 1996;2737–8.
[7] Mattei S, Seiler P, Diederich F, Gramlich V. Helvetica Chim Acta 1995;78:1904–11.
[8] Lhotak P, Shinkai S. Tetrahedron 1995;51:7681–96.
[9] James TD, Shinmori H, Takeuchi M, Shinkai S. Chem Commun 1996;705–6.
[10] Bar G, Rubin S, Cutts RW, Taylor TN, Zawodzinski Jr. TA. Langmuir 1995;12:1172–9.
[11] Bruening ML, Zhou Y, Aguilar G, Agee R, Bergbreiter DE, Crooks RM. Langmuir 1997;13:770–8.
[12] Bruening ML, Zhou Y, Zhao M, Crooks RM, Bergbreiter DE. Proc PMSE 1997;77:77–8.

[13] Liu Y, Zhao M, Bergbreiter DE, Crooks RM. J Am Chem Soc 1997;119:8720–1.
[14] Sheiko SS, Muzafarov AM, Winkler RG, Getmanova EV, Eckert G, Reineker P. Langmuir 1997;13:4172–81.
[15] Tsukruk VV, Rinderspacher F, Bliznyuk VN. Langmuir 1997;13:2171–6.
[16] Watanabe S, Regen SL. J Am Chem Soc 1994;116:8855–6.
[17] Zhou Y, Bruening ML, Bergbreiter DE, Crooks RM, Wells M. J Am Chem Soc 1996;118:3773–4.
[18] Zhou Y, Bruening ML, Liu Y, Crooks RM, Bergbreiter DE. Langmuir 1996;12:5519–21.
[19] Zhao M, Zhou Y, Bruening ML, Bergbreiter DE, Crooks RM. Langmuir 1997;13:1388–91.
[20] Wells M, Crooks RM. J Am Chem Soc 1996;118:3988–9.
[21] Brunner HJ. Organomet Chem 1995;500:39–46.
[22] Brunner H, Bublak P. Synthesis 1995;January:36–8.
[23] Butz T, Murer P, Seebach D. Proc PMSE 1997;77:132–3.
[24] Mak CC, Chow HF. Macromolecules 1997;30:1228–30.
[25] McElhanon JR, Wu MJ, Escobar M, McGrath DV. Macromolecules 1996;29:8979–82.
[26] McElhanon JR, Wu MJ, Escobar M, Chaudhry U, Hu CL, McGrath DV. J Org Chem 1997;62:908–15.
[27] Seebach D, Herrmann GF, Lengweiler UD, Bachmann BM, Amrein W. Angew Chem Int Ed Engl 1996;35:2795–7.
[28] Jansen JFGA, de Brabander-van den Berg EMM, Meijer EW. Science 1994;266:1226–9.
[29] Jansen JFGA, Meijer EW, de Branbander-Van den Berg EMM. J Am Chem Soc 1995;117:4417–8.
[30] Jansen JFGA, Janssen RAJ, de Branbander-Van den Berg EMM, Meijer EW. Adv Mater 1995;7:561–4.
[31] Miklis P, Çagin T, Goddard III WA. J Am Chem Soc 1997;119:7458–62.
[32] Lescanec RL, Muthukumar M. Macromolecules 1990;23:2280–8.
[33] Murat M, Grest GS. Macromolecules 1996;29:1278–85.
[34] Mansfield ML, Klushin LI. Macromolecules 1993;26:4262–68.
[35] Mansfield ML, Klushin LI. J Phys Chem 1992;96:3994–8.
[36] Carl W. J Chem Soc, Faraday Trans 1996;92:4151–4.
[37] Cai C, Chen ZY. Macromolecules 1997;30:5104–17.
[38] Chen ZY, Cui SM. Macromolecules 1996;29:7943–52.
[39] Boris D, Rubinstein M. Macromolecules 1996;29:7251–60.
[40] Wooley KL, Klug CA, Tasaki K, Schaefer J. J Am Chem Soc 1997;119:53–8.
[41] Gorman CB, Hager MW, Parkhurst BL, Smith JC. Macromolecules 1998;31:815–22.
[42] Naylor AM, Goddard III WA, Kiefer GE, Tomalia DA. J Am Chem Soc 1989;111:2339–41.
[43] Maple JA, Hwang MJ, Stockfisch TP, Dinur U, Waldman M, Ewig CS, Hagler AT. J Comput Chem 1994;15:162–82.
[44] Hwang MJ, Stockfisch TP, Hagler AT. J Am Chem Soc 1994;116:2515–25.
[45] Sun H, Mumby SJ, Maple JR, Hagler AT. J Am Chem Soc 1994;116:2978–87.
[46] Sun H. J Comput Chem 1994;15:752–68.
[47] Sun H. Macromolecules 1995;28:701–12.
[48] Humphrey W, Xu D, Sheves M, Schulten K. J Phys Chem 1995;99:14549–60.
[49] Shamovsky IL, Ross GM, Riopelle RJ, Weaver DF. J Am Chem Soc 1996;118:9743–9.
[50] Anderson HC. J Comp Phys 1983;52:24–34.
[51] Hawker CJ, Fréchet JMJ. J Am Chem Soc 1990;112:7638–47.
[52] Hawker CJ, Fréchet JMJ. J Am Chem Soc 1992;114:8405–13.
[53] Wooley KL, Hawker CJ, Fréchet JMJ. J Am Chem Soc 1991;113:4252–61.
[54] Xu Z, Moore JS. Angew Chem Int Ed Engl 1993;32:246–8.
[55] Bharathi P, Patel U, Kawaguchi T, Pesak DJ, Moore JS. Macromolecules 1995;28:5955–63.
[56] Xu Z, Kahr M, Walker KL, Wilkins CL, Moore JS. J Am Chem Soc 1994;116:4537–50.
[57] Kawaguchi T, Walker KL, Wilkins CL, Moore JS. J Am Chem Soc 1995;117:2159–65.
[58] Höger S, Spickermann J, Morrison DL, Dziezok P, Räder HJ. Macromolecules 1997;30:3110–11.
[59] Pesak DJ, Moore JS. Angew Chem Int Ed Engl 1997;36:1636–9.
[60] Kaneko T, Horie T, Asano M, Aoki T, Oikawa E. Macromolecules 1997;30:3118–21.
[61] Buchko CJ, Wilson PM, Xu Z, Zhang J, Moore JS, Martin DC. Polymer 1995;36:1817–25.
[62] Morgenroth F, Kübel C, Müllen K. J Mater Chem 1997;7:1207–11.
[63] Mourey TH, Turner SR, Rubinstein M, Fréchet JMJ, Hawker CJ, Wooley KL. Macromolecules 1992;25:2401–6.
[64] Hawker CJ, Wooley KL, Fréchet JMJ. J Am Chem Soc 1993;115:4375–6.
[65] Jiang DL, Aida T. Nature 1997;388:454–6.
[66] Tomoyose Y, Jiang DL, Jin RH, Aida T, Yamashita T, Horie K, Yashima E, Okamoto Y. Macromolecules 1996;29:5236–8.
[67] Gorman CB, Smith JC. Submitted for publication.
[68] Devadoss C, Bharathi P, Moore JS. Angew Chem Int Ed Engl 1997;36:1633–5.